Observational Study

Medicine®

OPEN

Identification and validation of a risk signature based on extracellular matrix-related genes in gliomas

Jia Liu, BM, Guilin Li, PhD*

Abstract

Gliomas have the highest incidence among primary brain tumors, and the extracellular matrix (ECM) plays a vital role in tumor progression. We constructed a risk signature using ECM-related genes to predict the prognosis of patients with gliomas.

mRNA and clinical data from glioma patients were downloaded from The Cancer Genome Atlas (TCGA), Genotype-Tissue Expression (GTEx) and Chinese Glioma Genome Atlas (CGGA) databases. Differentially expressed ECM-related genes were screened, and a risk signature was built using least absolute shrinkage and selection operator (LASSO) Cox regression. Cell type identification by estimating relative subsets of RNA transcripts (CIBERSORT) was used to assess immune infiltration in different risk groups. Gene set enrichment analysis (GSEA) was performed to explore the molecular mechanisms of the genes employed in the risk score.

Differentially expressed ECM-related genes were identified, and their associated regulatory mechanisms were predicted via analysis of protein–protein interaction (PPI), transcription factor (TF) regulatory and TF coexpression networks. The established risk signature considered 17 ECM-related genes. The prognosis of the high-risk group was significantly worse than that of the low-risk group. We used the CGGA database to validate the signature. CIBERSORT indicated that the levels of naive B cells, activated memory CD4 T cells, regulatory T cells, gamma delta T cells, activated NK cells, monocytes, activated dendritic cells and activated mast cells were higher in the high-risk group. The levels of plasma cells, CD8 T cells, naive CD4 T cells, resting memory CD4 T cells, M0 macrophages, M1 macrophages, resting mast cells, and neutrophils were lower in the high-risk group. Ultimately, GSEA showed that the terms intestinal immune network for IgA production, primary immunodeficiency, and ECM receptor interaction were the top 3 terms enriched in the high-risk group. The terms Wnt signaling pathway, ErbB signaling pathway, mTOR signaling pathway, and calcium signaling pathway were enriched in the low-risk group.

We built a risk signature to predict glioma prognosis using ECM-related genes. By evaluating immune infiltration and biofunctions, we gained a further understanding of this risk signature. This risk signature could be an effective tool for predicting glioma prognosis.

This study did not require ethical approval. We will disseminate our findings by publishing results in a peer-reviewed journal.

Abbreviations: CGGA = Chinese Glioma Genome Atlas, DEGs = differentially expressed genes, ECM = extracellular matrix, FDR = false discovery rate, GTEx = Genotype-Tissue Expression, IDH = isocitrate dehydrogenase, LASSO = least absolute shrinkage and selection operator, OS = overall survival, PPI = protein–protein interaction, ROC = receiver operating characteristic, STRING = Search Tool for the Retrieval of Interacting Genes/Proteins, TCGA = The Cancer Genome Atlas.

Keywords: extracellular matrix, gliomas, GSEA, immune cell infiltration, prognosis, risk

1. Introduction

The extracellular matrix (ECM), which constitutes scaffolds of tissues and organs, is a complex network composed of more than 300 proteins (with main components including extracellular proteins, proteoglycans, and glycoproteins).[1–3] The ECM could also regulate cell growth, differentiation, migration, vascular

Editor: YX Sun.

This study was supported by grants from the National Natural Science Foundation of China (81860217, 81560219 and 81200853), a grant from the Key Research and Development Program of Jiangxi Province, China (20192BBH80017), and a grant from the Natural Science Foundation of Jiangxi Province, China (20171BAB205025).

Patient consent for publication was not required.

The authors have no conflicts of interest to disclose.

Data sharing is not applicable to this article, as all the data were obtained from a publicly available database.

The datasets generated during and/or analyzed during the current study are publicly available.

Queen Mary School, Medical School of Nanchang University, Nanchang, Jiangxi, PR China.

** Correspondence: Guilin Li, Department of Physiology, Medical School of Nanchang University, 461 Bayi Road, Nanchang 330006, Jiangxi, PR China (e-mail: liguilin@ncu.edu.cn).*

How to cite this article: Liu J, Li G. Identification and validation of a risk signature based on extracellular matrix-related genes in gliomas. Medicine 2021;100:16 (e25603).

Received: 26 December 2020 / Received in final form: 28 March 2021 / Accepted: 1 April 2021

http://dx.doi.org/10.1097/MD.0000000000025603

development, and immune function.[4,5] As the key to maintaining tissue homeostasis, the ECM is a dynamic environment, and ECM disorders can promote tumor occurrence, progression, and metastasis.[6,7] The ECM could act as a physical barrier between tumor cells and normal cells in the early stage of tumors, preventing tumor cell invasion.[8] However, under the influence of many factors (such as hypoxia, metabolic stress, and tumor cell proliferation), the remodeling process of the ECM is gradually deregulated, which is manifested by increased deposition (fibrosis) and the degradation of ECM.[9] It was reported that the degradation of ECM was an important step in tumor invasion and metastasis, and MMP9 (a matrix-degrading enzyme) was overexpressed in highly aggressive breast cancer and was closely related to recurrence.[10,11] In addition, ECM deposition was found in solid tumors (fibrosis), making tumor tissues stiffer than normal tissues and activating the proliferation of tumor cells.[12,13] Additionally, increased expression of ECM-related genes was associated with poor prognosis in clear cell renal cell carcinoma, and the upregulated expression of genes that mediate ECM remodeling could improve the mortality of breast cancer, lung cancer, and gastric cancer.[14,15]

The incidence of gliomas is highest among primary brain tumors.[16] Gliomas include astrocytoma, oligodendroglioma, oligoastrocytoma, ependymoma, malignant glioma, etc.[17] Gliomas are classified into 4 grades (grade I-IV) by the World Health Organization (WHO).[18] Although surgical resection, radiotherapy, and chemotherapy are the main treatments for gliomas, the prognosis is still poor.[19,20] Glioblastoma (part of astrocytoma, grade IV) accounts for 50% of gliomas and generally responds poorly to all therapies, leading to the highest mortality rate, with a median survival time of approximately 1 to 2 years.[21,22] It is confusing that the prognosis of patients with low-grade glioma is quite different; some patients have a poor prognosis, while some patients could survive for more than 10 years.[23] Currently, a study indicated that isocitrate dehydrogenase (IDH) mutation and 1p/19q codeletion could serve as important biomarkers for predicting the prognosis and development of gliomas, but these biomarkers were only effective in some patients.[24] Therefore, it is essential to confirm biomarkers that can reliably predict the prognosis of glioma patients and develop more effective targeted drugs to guide the treatment of gliomas. Increasing studies have revealed the relationship between the ECM and gliomas, and ECM remodeling could accelerate the cell proliferation, angiogenesis, invasion, and infiltration of gliomas; thus, the ECM is the focus of our research.[25–27]

In our study, we used the mRNA expression data obtained from The Cancer Genome Atlas (TCGA) database and the Genotype-Tissue Expression (GTEx) database to screen differentially expressed genes (DEGs) from ECM-related genes. Then, a risk signature was constructed to predict the prognosis of patients with gliomas using ECM-related genes. A microarray dataset obtained from the Chinese Glioma Genome Atlas (CGGA) database was used to validate the accuracy of the risk signature. Finally, risk score-related immune cell infiltration and potential biological functions were also evaluated.

2. Materials and methods

2.1. Data collection

The mRNA expression data and clinical data of patients with gliomas (including low-grade glioma and glioblastoma) in the TCGA database were obtained from UCSC Xena (http://xena.ucsc.edu/). The mRNA expression of normal brain tissues was downloaded from the GTEx database (http://commonfund.nih.gov/GTEx/). The transcriptome data from TCGA and GTEx (702 glioma tissues and 1152 normal brain tissues) were merged for further analysis (training set). ECM-related genes were found in 2 ECM-related gene sets ("KEGG ECM RECEPTOR INTERACTION" and "KEGG FOCAL ADHESION") from the Molecular Signatures Database (MSigDB) (https://www.gsea-msigdb.org/gsea/msigdb/index.jsp). Data from 1018 patients with gliomas in CGGA (http://www.cgga.org.cn/) were also obtained to validate the risk signature (validation set). Intersecting ECM-related genes in the training set and validation set were screened. To explore regulatory mechanisms, we also acquired information on transcription factors (TFs) from the Cistrome Cancer database (http://cistrome.org/).[28]

2.2. DEGs

DEGs were identified from intersecting genes in the training set via the limma package in R software.[29] Differentially expressed TFs were also identified. A protein-protein interaction (PPI) network was constructed with the Search Tool for the Retrieval of Interacting Genes/Proteins (STRING) database (score >0.4) (https://stringdb.org/) to assess the relationships among the DEGs. Through cluster analysis, subnets were visualized from the PPI network. TF enrichment analysis was performed via the Database for Annotation, Visualization and Integrated Discovery (DAVID) website (https://david.ncifcrf.gov/) to construct a TF-DEG regulatory network ($P < .05$).

2.3. The risk signature

Univariable Cox regression was conducted to identify the DEGs related to prognosis ($P < .05$). We used DEGs related to prognosis and differentially expressed TFs to establish a coexpression network (P value $< .05$ and correlation coefficient > 0.4 were defined as the cutoff criteria). Then, the risk signature was built using the selected DEGs related to prognosis via least absolute shrinkage and selection operator (LASSO) Cox regression, and the risk score was calculated. Based on the median value of the risk score, the glioma patients were divided into 2 groups (high risk and low risk). The accuracy of the risk signature was estimated via a receiver operating characteristic (ROC) curve. Kaplan–Meier survival curves were used to compare the overall survival (OS) between the high-risk group and the low-risk group (the log-rank test). Then, univariable and multivariable Cox regression analyses were performed to evaluate whether the risk score was an independent predictor of poor OS in glioma patients. Finally, the CGGA database was used to validate the signature.

2.4. Immune cell infiltration

Cell type identification by estimating relative subsets of RNA transcripts (CIBERSORT) was used to evaluate the infiltration of immune cells. Through this deconvolution algorithm based on gene expression profiles, we could clarify the relationship between the risk score and the infiltration of 22 immune cells (including naive B cells, memory B cells, plasma cells, CD8 T cells, naive CD4 T cells, and resting memory CD4 T cells, among others).[30–32]

2.5. Gene set enrichment analysis (GSEA)

GSEA was conducted to assess the molecular mechanisms of the genes in the risk score. We downloaded the gene set "c2.cp.kegg.

Table 1

Characteristics of the patients obtained from the TCGA and CGGA database.

Basic information	TCGA (n=615)	CGGA (n=696)
Age	45 (median)	43 (median)
Gender		
Female	267	289
Male	348	407
Grade		
WHO I&II	–	182
WHO III&IV	–	514
Radiotherapy		
Yes	421	550
No	194	146
Chemotherapy		
Yes	–	505
No	–	191
IDH mutation		
Mutant	–	376
Wildtype	–	320
1p19q Codeletion		
Yes	–	145
No	–	551
MGMTp methylation		
Yes	–	389
No	–	307

CGGA = The Chinese Glioma Genome Atlas, IDH = isocitrate dehydrogenase, TCGA = The Cancer Genome Atlas.

v7.1.symbols" from MSigDB for GSEA. Normalized enrichment scores, nominal *P* values (NOM P values) and false discovery rate (FDR) Q values were acquired though GSEA. A NOM *P* value <.05 and an FDR Q value of <0.25 were considered significantly enriched.

2.6. Statistical analysis

We performed the log-rank test and Cox regression via the survival package for R. The LASSO Cox regression was carried out via the glmnet package for R. The ROC curves were generated via the survival ROC package for R. All networks were displayed via Cytoscape software version 3.8.0.

3. Results

3.1. DEGs

The basic clinical information of the glioma patients in the TCGA and CGGA databases is shown in Table 1. We identified 89 DEGs from the intersecting ECM-related genes; 52 of the DEGs exhibited upregulated expression, and 37 exhibited down-

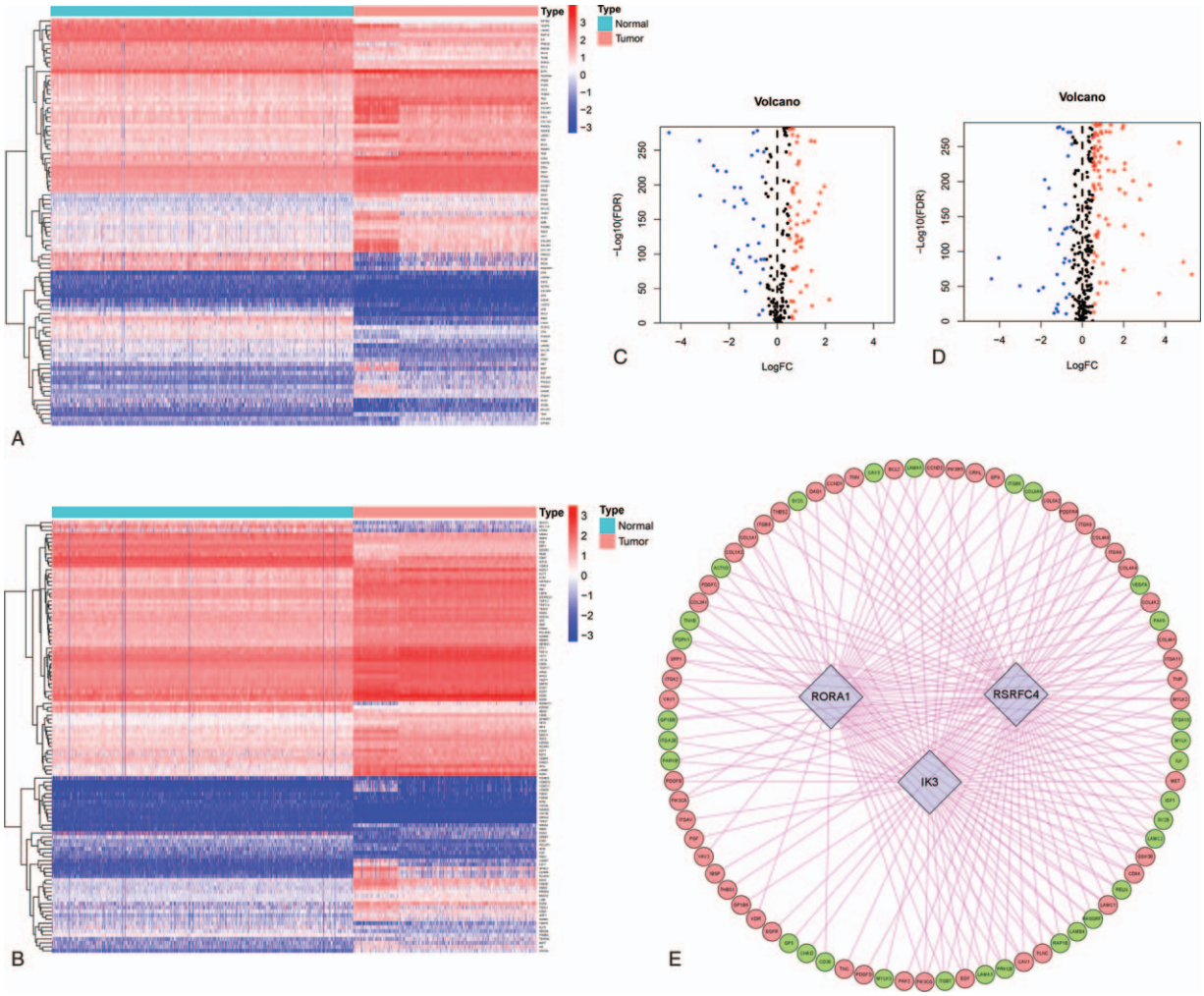

Figure 1. DEGs. Differentially expressed ECM-related genes between glioma tissues and normal brain tissues from the TCGA database were illustrated using a heatmap (A) and volcano plot (C). Differentially expressed TFs between gliomas and normal brain tissues were identified and are shown via a heatmap (B) and volcano plot (D). A TF-DEG regulatory network was constructed (E). Diamond nodes represent enriched TFs, red circular nodes represent upregulated DEGs, and green circular nodes represent downregulated DEGs. DEGs = differentially expressed genes, ECM = extracellular matrix, TCGA = The Cancer Genome Atlas, TF = transcription factor.

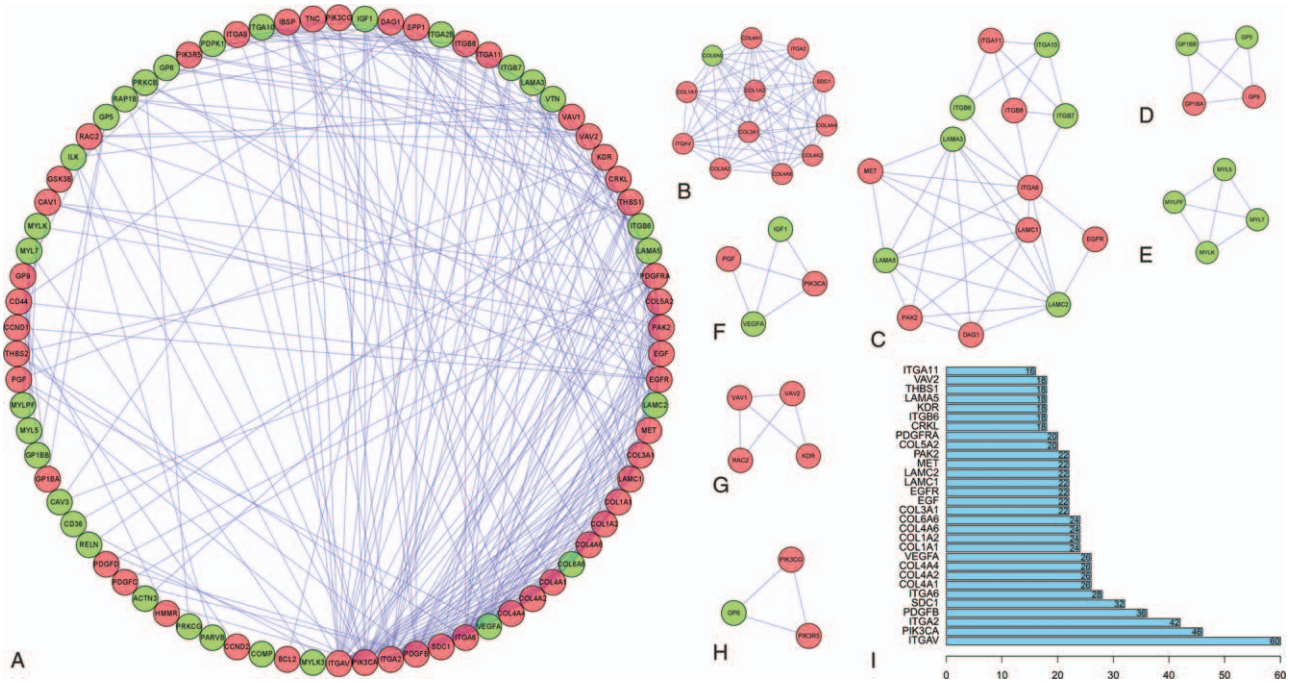

Figure 2. PPI network. A PPI network was established based on the DEGs via the STRING database (A). Through cluster analysis, subnets were visualized from the PPI network (B-H). Red circular nodes represent upregulated DEGs, and green circular nodes represent downregulated DEGs. By counting the number of edges connected to the nodes, ITGAV was identified as the hub gene. DEGs = differentially expressed genes, ITGAV = integrin subunit alpha V, PPI = protein–protein interaction.

regulated expression (Fig. 1A and C). In addition, 289 differentially expressed TFs were screened; 193 exhibited upregulated expression, and 96 exhibited downregulated expression (Fig. 1B and D). A TF regulatory network was constructed based on the 89 DEGs and enriched TFs (Fig. 1E). A PPI network and subnets obtained through cluster analysis were established and showed that integrin subunit alpha V (ITGAV) was the hub gene (Fig. 2A-I).

3.2. The risk signature

We performed univariate Cox regression to identify the DEGs related to prognosis (Fig. 3A). A TF coexpression network was constructed based on the 79 DEGs related to prognosis and 289 differentially expressed TFs (Fig. 3B). The risk signature was built using the selected genes via LASSO Cox regression, and the risk score was calculated (Table 2) (Fig. 4A-C). Based on the median value of the risk score, the glioma patients were divided into 2 groups (high risk and low risk). The ROC curve results showed that the OS of patients with gliomas was well predicted by the risk score [area under the curve (AUC) at 1 year = 0.884, AUC at 3 years = 0.926, AUC at 5 years = 0.871] (Fig. 4D). The survival curve suggested that the prognosis of the high-risk group was significantly worse than that of the low-risk group ($P < .001$) (Fig. 4E). Univariable Cox regression showed that age [hazard ratio (HR) = 1.066, 95% confidence interval (CI) = 1.055–1.076, $P < .001$], gender (HR = 1.298, 95% CI = 1.005–1.667, $P = .046$), radiation therapy (HR = 2.243, 95% CI = 1.608–3.130, $P < .001$) and risk score (HR = 3.493, 95% CI = 3.055–3.995, $P < .001$) were closely related to poor prognosis in gliomas (Fig. 4F). The risk score was also identified as a factor associated with prognosis (HR = 3.014, 95% CI = 2.552–3.560, $P < .001$) via multivariable Cox regression (Fig. 4G). We also established a nomogram that could predict the survival probability of 1-year, 3-year and 5-year OS (Fig. 4H). The calibration curve revealed the accuracy of the prediction using the nomogram (Fig. 4I). The CGGA database was used to validate the risk signature. The patients were divided into 2 groups (Fig. 5A-C). The ROC curve results showed that the OS of patients with gliomas was well predicted by the risk score (AUC at 1 year = 0.748, AUC at 3 years = 0.802, AUC at 5 years = 0.806] (Fig. 5D). The survival curve also suggested that the prognosis of the high-risk group was significantly worse than that of the low-risk group ($P < .001$) (Fig. 5E). Univariable Cox regression showed that age (HR = 1.029, 95% CI = 1.021–1.036, $P < .001$), chemotherapy (HR = 1.290, 95% CI = 1.059–1.571, $P = .011$), IDH mutation (HR = 0.336, 95% CI = 0.281–0.401, $P < .001$), 1p19q codeletion (HR = 0.237, 95% CI = 0.179–0.315, $P < .001$), grade (HR = 4.841, 95% CI = 3.754–6.242, $P < .001$) and risk score (HR = 2.034, 95% CI = 1.869–2.214, $P < .001$) were closely related to poor prognosis in gliomas (Fig. 5F). The risk score was also identified as a factor associated with prognosis (HR = 1.439, 95% CI = 1.278–1.620, $P < .001$) via multivariable Cox regression (Fig. 5G). The nomogram could predict the survival probability of 1-year, 3-year, and 5-year OS (Fig. 5H). The calibration curve revealed the accuracy of the prediction using the nomogram (Fig. 5I).

3.3. Evaluation of immune cell infiltration

CIBERSORT was used to evaluate the relationship between immune cell infiltration and the risk score. The levels of naive B cells ($P = .002$), activated memory CD4 T cells ($P < .001$), regulatory T

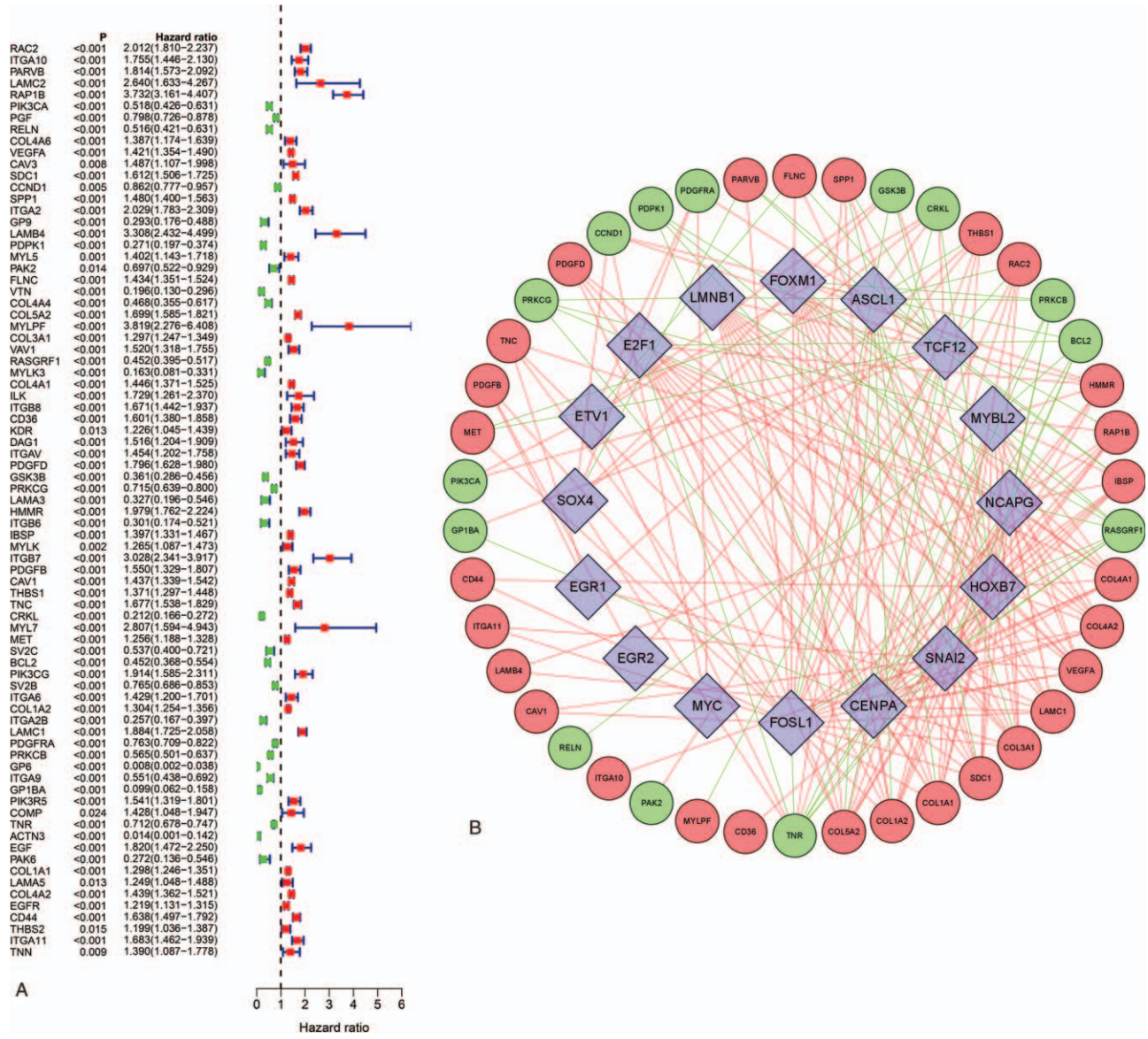

Figure 3. DEGs and prognosis. DEGs related to prognosis were screened via univariate Cox regression (A). A coexpression network was established using differentially expressed TFs and DEGs related to prognosis (B). Diamond nodes represent TFs, red circular nodes represent high-risk DEGs (HR > 1), green circular nodes represent low-risk DEGs (HR < 1), red edges represent positive regulation, and green edges represent negative regulation. DEGs = differentially expressed genes, HR = hazard ratio, TF = transcription factor.

Table 2

The coefficients of included genes obtained from LASSO Cox regression.

Gene	Coefficient
PARVB	0.0962
RAP1B	0.0529
PIK3CA	−0.0132
PGF	−0.0604
VEGFA	0.0294
SDC1	0.1073
SPP1	0.1006
FLNC	0.0940

LASSO = least absolute shrinkage and selection operator.

cells ($P < .001$), gamma delta T cells ($P < .001$), activated NK cells ($P = 0.012$), monocytes ($P < .001$), activated dendritic cells ($P < .001$) and activated mast cells ($P < .001$) were higher in the high-risk group than in the low-risk group. The levels of plasma cells ($P = .001$), CD8 T cells ($P = .002$), naive CD4 T cells ($P < .001$), resting memory CD4 T cells ($P < .001$), M0 macrophages ($P < .001$), M1 macrophages ($P < .001$), resting mast cells ($P = .004$), and neutrophils ($P < .001$) were lower in the high-risk group than in the low-risk group (Fig. 6A). Then, we found that the expression of programmed cell death 1 (PD-1; correlation coefficient = 0.38, $P < .001$), programmed cell death 1 ligand 1 (PD-L1; correlation coefficient = 0.55, $P < .001$), lymphocyte activating 3 (LAG3; correlation coefficient = 0.17, $P < .001$), hepatitis A virus cellular receptor 2 (HAVCR2, correlation coefficient = 0.55, $P < .001$), B- and T-lymphocyte–associated

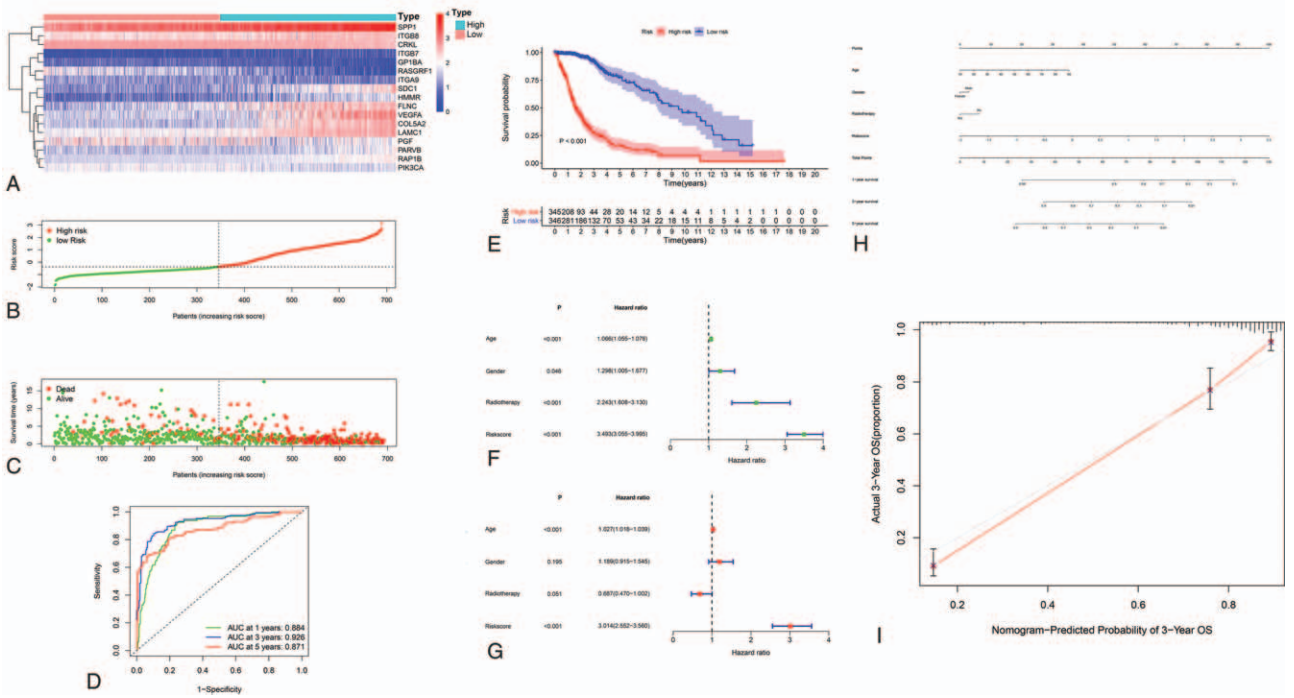

Figure 4. The risk signature. The expression of selected ECM-related genes in different groups (A). The distribution of patients with gliomas into different groups (B). Survival status of the patients in different groups (C). The AUC of the ROC curve is shown (D). Kaplan-Meier survival analysis revealed that a high risk score was significantly related to poor OS (E). Univariate Cox regression and multivariate Cox regression demonstrated that the risk score was an independent prognostic factor in gliomas (F-G). The results of the nomogram and the calibration curve implied that the accuracy of the signature was satisfactory (H). AUC = area under the curve, ECM = extracellular matrix, OS = overall survival, ROC = receiver operating characteristic.

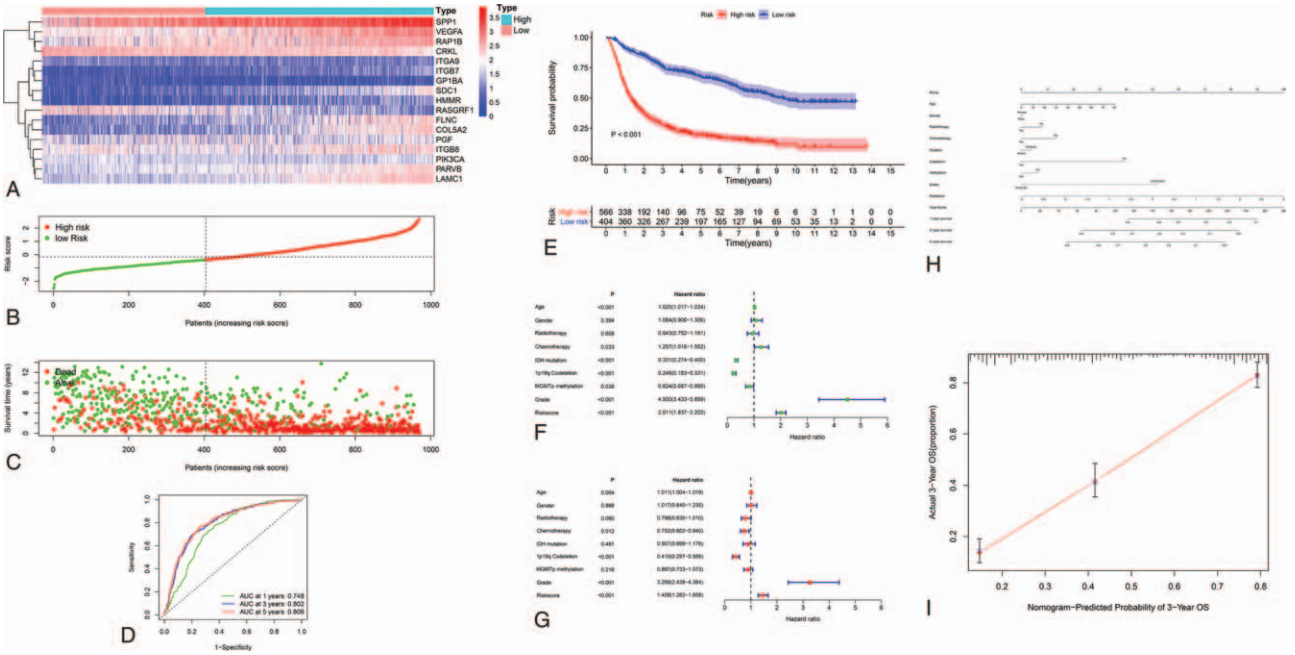

Figure 5. Validation using the CGGA database. The expression of selected ECM-related genes in different groups (A). The distribution of patients with gliomas into different groups (B). Survival status of the patients in different groups (C). The AUC of the ROC curve is shown (D). Kaplan–Meier survival analysis revealed that a high risk score was significantly related to poor OS (E). Univariate Cox regression and multivariate Cox regression demonstrated that the risk score was an independent prognostic factor in gliomas (F-G). The results of the nomogram and the calibration curve implied that the accuracy of the signature was satisfactory (H). AUC = area under the curve, CGGA = the Chinese Glioma Genome Atlas, ECM = extracellular matrix, OS = overall survival, ROC = receiver operating characteristic.

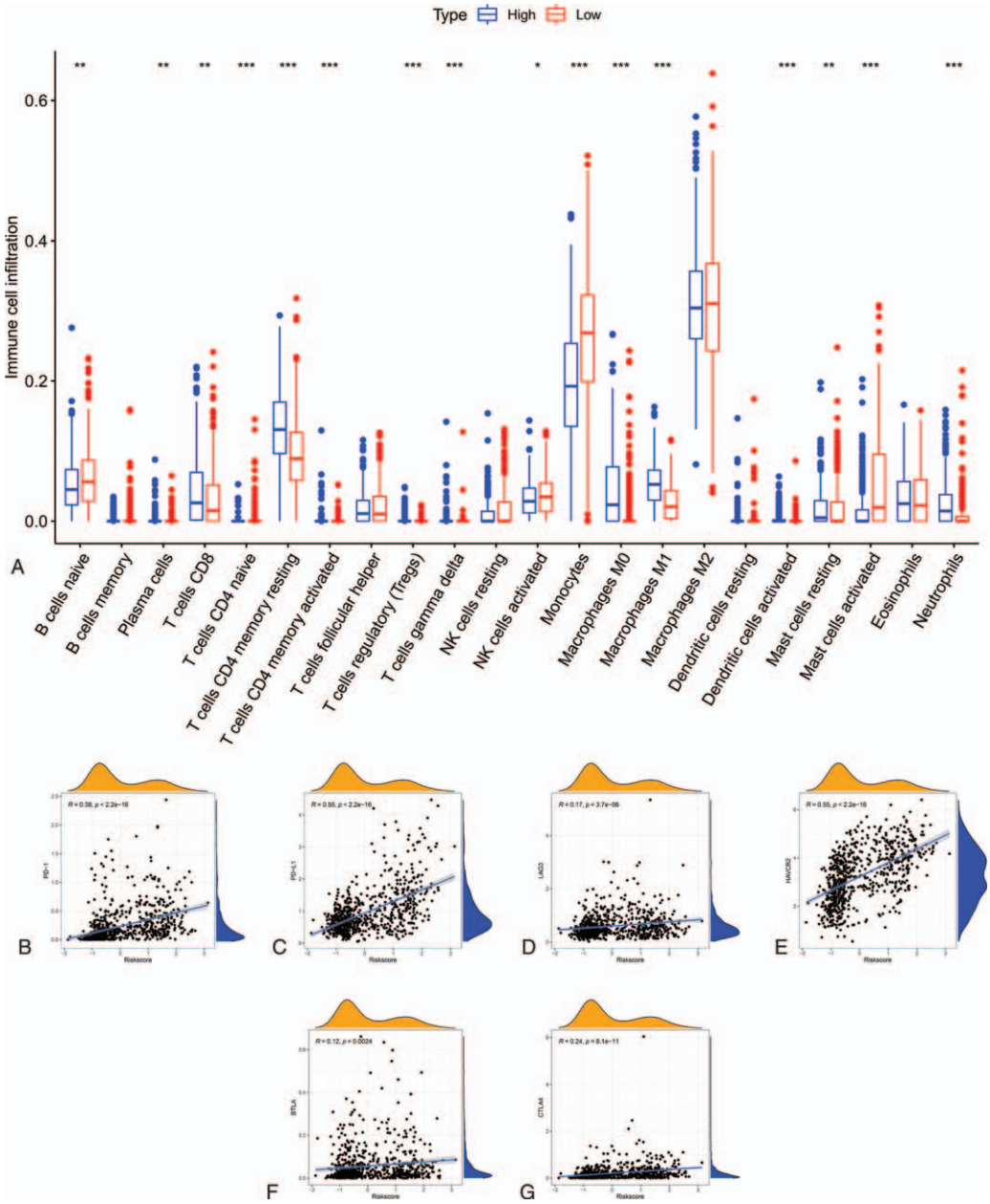

Figure 6. Immune cell infiltration. CIBERSORT was used to evaluate the immune cell infiltration in different risk groups (A). The risk score was significantly positively correlated with the expression of immune checkpoints (PD-1, PD-L1, LAG3, HAVCR2, BTLA, and CTLA4) (B-G). BTLA = B- and T-lymphocyte–associated, CTLA4 = cytotoxic T-lymphocyte–associated protein 4, HAVCR2 = hepatitis A virus cellular receptor 2, LAG3 = lymphocyte activating 3, PD-1 = programmed cell death 1, PD-L1 = programmed cell death 1 ligand 1.

(BTLA, correlation coefficient = 0.12, $P = .002$), and cytotoxic T-lymphocyte–associated protein 4 (CTLA4, correlation coefficient = 0.24, $P < .001$) was significantly positively correlated with the risk score (Fig. 6B-G).

3.4. GSEA

GSEA was conducted to explore the biofunctions of the genes related to the risk score. The most significantly enriched signaling pathways in the high-risk group are shown in Table 3. The most significant signaling pathways enriched in the low-risk group are shown in Table 4.

4. Discussion

Gliomas account for 80% of primary brain malignancies, and the 5-year survival rate is less than 10%.[33,34] In the past decade, targeted therapies for the treatment of glioma have been rapidly developed, but the effects have not been satisfactory.[35] Recent studies have pointed out that the ECM plays an important role in tumors. The ECM could have an impact on metastatic glioma cells.[36] ECM signaling could drive the proliferation, differentiation, and invasion and defer the apoptosis of tumor cells.[37] Therefore, we identified ECM-related genes in gliomas as

Table 3

Gene sets enriched in the high risk phenotype.

Gene set name	NES	NOM *p*-value	FDR *q*-value
KEGG_INTESTINAL_IMMUNE_NETWORK_FOR_IGA_PRODUCTION	1.9214	.0000	0.0353
KEGG_PRIMARY_IMMUNODEFICIENCY	1.8421	.0039	0.0322
KEGG_ECM_RECEPTOR_INTERACTION	1.9250	.0040	0.0387
KEGG_P53_SIGNALING_PATHWAY	1.8972	.0041	0.0348
KEGG_TOLL_LIKE_RECEPTOR_SIGNALING_PATHWAY	1.8063	.0079	0.0311
KEGG_ANTIGEN_PROCESSING_AND_PRESENTATION	1.8832	.0080	0.0315
KEGG_JAK_STAT_SIGNALING_PATHWAY	1.7603	.0098	0.0380
KEGG_FOCAL_ADHESION	1.8111	.0120	0.0319
KEGG_CELL_ADHESION_MOLECULES_CAMS	1.8061	.0139	0.0302
KEGG_CYTOSOLIC_DNA_SENSING_PATHWAY	1.7429	.0154	0.0396
KEGG_NATURAL_KILLER_CELL_MEDIATED_CYTOTOXICITY	1.7479	.0158	0.0402
KEGG_APOPTOSIS	1.7449	.0160	0.0400
KEGG_RIG_I_LIKE_RECEPTOR_SIGNALING_PATHWAY	1.5169	.0434	0.1215

FDR = false discovery rate, NES = normalized enrichment score, NOM = nominal.
Gene sets with NOM *p*-val < .05 and FDR *q*-val < 0.25 were considered significant.

research targets to discover the molecular mechanism of glioma progression and therapeutic biomarkers.

Here, we analyzed the relationship between ECM-related genes and the prognosis of gliomas in detail. Additionally, the risk score we calculated based on 17 selected genes was an independent factor leading to the poor prognosis of gliomas. Numerous studies have revealed a close relationship between the 17 genes included in the risk signature and the development of tumors. The overexpression of PARVB increased the capability of cell migration in tongue squamous cell carcinoma, but PARVB was considered a metastasis suppressor in urothelial cell carcinoma.[38,39] Some microRNAs reduced the ability of tumor metastasis by negatively regulating RAP1B.[40–42] In triple-negative breast cancer, the expression of PIK3CA could be a better prognostic marker independent of subtype.[43] Studies have confirmed that the knockdown of SERPINE1 and upregulation of microRNA-29c downregulate the expression of VEGFA to promote cell apoptosis in tumors.[44,45] Lower expression of SDC1 could lead to an increased metastasis rate in gallbladder cancer through the ERK/Snail pathway.[46] These selected ECM-related genes are worthy of further investigation as targets for glioma treatments.

The results of CIBERSORT indicated that the levels of immune cell infiltration were significantly associated with the risk score. Activated CD8 T cells are an important member of the immune response against tumors, and high levels of CD8 T cells, not CD4 T cells, could improve the survival rate of patients with gliomas.[47–49] CD4 T cells are conducive to the angiogenesis and tumor progression of gliomas.[50] However, we found that some immune cells that exerted antitumor responses were significantly upregulated in the risk group but led to a poor prognosis. The reasons are very complicated. The first is the expansion of immunosuppressive cells, such as regulatory T cells, which makes the immune response ineffective, and gliomas themselves also have a strong immunosuppressive effect.[51,52] Additionally, new findings suggest that tumor cells can escape the immune response by using immune checkpoints.[53] The results of our study implied that the risk score was significantly positively correlated with the expression of immune checkpoints, indicating that the immunosuppressive effect of the high-risk group was stronger. We believe that it is vital to identify the connection between the ECM and immune cells in glioma, which could provide preliminary evidence for glioma immunotherapy.

Most of the pathways revealed by GSEA are related to the immune response and tumor cell migration and invasion, including primary immunodeficiency, the Wnt signaling pathway and the mTOR signaling pathway,[54–56] and suggest that their molecular mechanisms and biological functions are closely related to the risk score.

We should also realize that our research still has some limitations. First, the transcriptome data of normal brain tissue were lacking in the TCGA database, so we had to merge the transcriptome data of the 2 databases (TCGA database and GTEx database) for the identification and subsequent analysis of DEGs, which might cause errors. Second, there are few types of clinical data on gliomas in the TCGA database, which might lead to incomplete results. Third, research on the relationship between the risk score and immune cell infiltration functions has not been conducted in depth. Additionally, the biological functions of the genes related to the risk score were not further verified by basic experiments.

Table 4

Gene sets enriched in low risk phenotype.

Gene set name	NES	NOM *p*-value	FDR *q*-value
KEGG_WNT_SIGNALING_PATHWAY	−1.7562	.0080	0.1882
KEGG_ERBB_SIGNALING_PATHWAY	−1.7468	.0154	0.1266
KEGG_MTOR_SIGNALING_PATHWAY	−1.6935	.0201	0.1489
KEGG_CALCIUM_SIGNALING_PATHWAY	−1.7540	.0265	0.1608

FDR = false discovery rate, NES = normalized enrichment score, NOM = nominal.
Gene sets with NOM *p*-val < .05 and FDR *q*-val < 0.25 are considered as significant.

5. Conclusions

In conclusion, we built a risk signature to predict the prognosis of gliomas using ECM-related genes. Through the evaluation of immune infiltration and biofunctions, we have a further understanding of this risk signature. We believe that this risk signature could be an effective tool for predicting the prognosis of gliomas. In the future, ECM-related genes could become therapeutic targets for gliomas.

Author contributions

Conceptualization: Guilin Li.
Data curation: Jia Liu.
Formal analysis: Jia Liu.
Funding acquisition: Guilin Li.
Investigation: Jia Liu.
Methodology: Jia Liu, Guilin Li.
Resources: Guilin Li.
Software: Jia Liu, Guilin Li.
Writing – original draft: Jia Liu.
Writing – review & editing: Jia Liu, Guilin Li.

References

[1] Eble JA, Niland S. The extracellular matrix in tumor progression and metastasis. Clin Exp Metastasis 2019;36:171–98.
[2] Naba A, Clauser KR, Hoersch S, et al. The matrisome: in silico definition and in vivo characterization by proteomics of normal and tumor extracellular matrices. Mol Cell Proteomics 2012;11: M111.014647.
[3] Frantz C, Stewart KM, Weaver VM. The extracellular matrix at a glance. J Cell Sci 2010;123(Pt 24):4195–200.
[4] Mammoto T, Ingber DE. Mechanical control of tissue and organ development. Development 2010;137:1407–20.
[5] Pickup MW, Mouw JK, Weaver VM. The extracellular matrix modulates the hallmarks of cancer. EMBO reports 2014;15:1243–53.
[6] Quail DF, Joyce JA. Microenvironmental regulation of tumor progression and metastasis. Nat Med 2013;19:1423–37.
[7] Hynes RO. The extracellular matrix: not just pretty fibrils. Science (New York, NY) 2009;326:1216–9.
[8] Wu TH, Yu MC, Chen TC, et al. Encapsulation is a significant prognostic factor for better outcome in large hepatocellular carcinoma. J Surg Oncol 2012;105:85–90.
[9] Sala M, Ros M, Saltel F. A Complex and evolutive character: two face aspects of ecm in tumor progression. Front Oncol 2020;10:1620.
[10] Zhang Y, Qin L, Ma X, et al. Coexpression of matrix metalloproteinase-7 and tissue inhibitor of metalloproteinase-1 as a prognostic biomarker in gastric cancer. Dis Markers 2020;2020:8831466.
[11] Yousef EM, Tahir MR, St-Pierre Y, et al. MMP-9 expression varies according to molecular subtypes of breast cancer. BMC Cancer 2014; 14:609.
[12] Gilkes DM, Semenza GL, Wirtz D. Hypoxia and the extracellular matrix: drivers of tumour metastasis. Nat Rev Cancer 2014;14:430–9.
[13] Lu P, Weaver VM, Werb Z. The extracellular matrix: a dynamic niche in cancer progression. J Cell Biol 2012;196:395–406.
[14] Chang HY, Nuyten DS, Sneddon JB, et al. Robustness, scalability, and integration of a wound-response gene expression signature in predicting breast cancer survival. Proc Natl Acad Sci U S A 2005;102:3738–43.
[15] Chang HY, Sneddon JB, Alizadeh AA, et al. Gene expression signature of fibroblast serum response predicts human cancer progression: similarities between tumors and wounds. PLoS Biol 2004;2:E7.
[16] Ji X, Zhang H, Cui Q. A Panel of Synapse-Related Genes as a Biomarker for Gliomas. Front Neurosci 2020;14:822.
[17] Ostrom QT, Gittleman H, Xu J, et al. CBTRUS Statistical Report: Primary Brain and Other Central Nervous System Tumors Diagnosed in the United States in 2009-2013. Neuro Oncol 2016;18(suppl_5):v1–75.
[18] Wesseling P, Capper D. WHO 2016 Classification of gliomas. Neuropathol Appl Neurobiol 2018;44:139–50.
[19] Siegel R, Ma J, Zou Z, et al. Cancer statistics, 2014. CA 2014;64:9–29.
[20] Buckner JC, Brown PD, O'Neill BP, et al. Central nervous system tumors. Mayo Clin Proc 2007;82:1271–86.
[21] Caldarella A, Barchielli A. Glioblastoma in the Canton of Zurich, Switzerland revisited: 2005 to 2009. Cancer 2016;122:3740.
[22] Wu X, Hou P, Qiu Y, et al. Large-scale analysis reveals the specific clinical and immune features of DGCR5 in glioma. Onco Targets Ther 2020;13:7531–43.
[23] Rudà R, Soffietti R. Controversies in management of low-grade gliomas in light of new data from clinical trials. Neuro Oncol 2017;19:143–4.
[24] Aibaidula A, Chan AK, Shi Z, et al. Adult IDH wild-type lower-grade gliomas should be further stratified. Neuro Oncol 2017;19:1327–37.
[25] Ferrer VP, Moura Neto V, Mentlein R. Glioma infiltration and extracellular matrix: key players and modulators. Glia 2018;66:1542–65.
[26] Shimizu T, Kurozumi K, Ishida J, et al. Adhesion molecules and the extracellular matrix as drug targets for glioma. Brain Tumor Pathol 2016;33:97–106.
[27] Ulrich TA, de Juan Pardo EM, Kumar S. The mechanical rigidity of the extracellular matrix regulates the structure, motility, and proliferation of glioma cells. Cancer Res 2009;69:4167–74.
[28] Mei S, Meyer CA, Zheng R, et al. Cistrome cancer: a web resource for integrative gene regulation modeling in cancer. Cancer Res 2017;77: e19–22.
[29] Ritchie ME, Phipson B, Wu D, et al. limma powers differential expression analyses for RNA-sequencing and microarray studies. Nucleic Acids Res 2015;43:e47.
[30] Newman AM, Liu CL, Green MR, et al. Robust enumeration of cell subsets from tissue expression profiles. Nat Method 2015;12:453–7.
[31] Ye L, Zhang T, Kang Z, et al. Tumor-infiltrating immune cells act as a marker for prognosis in colorectal cancer. Front Immunol 2019;10:2368.
[32] Zhang L, Zhu P, Tong Y, et al. An immune-related gene pairs signature predicts overall survival in serous ovarian carcinoma. Onco Targets Ther 2019;12:7005–14.
[33] Ostrom QT, Gittleman H, Truitt G, et al. CBTRUS Statistical Report: Primary Brain and Other Central Nervous System Tumors Diagnosed in the United States in 2011-2015. Neuro Oncol 2018;20(suppl_4):iv1–86.
[34] Ostrom QT, Cote DJ, Ascha M, et al. Adult glioma incidence and survival by race or ethnicity in the United States from 2000 to 2014. JAMA Oncol 2018;4:1254–62.
[35] Zhou W, Liu X, van Wijnbergen JWM, et al. Identification of PIEZO1 as a potential prognostic marker in gliomas. Scientific Rep 2020;10:16121.
[36] Vollmann-Zwerenz A, Leidgens V, Feliciello G, et al. Tumor cell invasion in glioblastoma. Int J Mol Sci 2020;21:1932.
[37] Walker C, Mojares E, Del Río Hernández A. Role of extracellular matrix in development and cancer progression. Int J Mol Sci 2018;19:3028.
[38] Eslami A, Miyaguchi K, Mogushi K, et al. PARVB overexpression increases cell migration capability and defines high risk for endophytic growth and metastasis in tongue squamous cell carcinoma. Br J Cancer 2015;112:338–44.
[39] Wu CF, Ng KF, Chen CS, et al. Expression of parvin-beta is a prognostic factor for patients with urothelial cell carcinoma of the upper urinary tract. Br J Cancer 2010;103:852–60.
[40] Fan M, Ma X, Wang F, et al. MicroRNA-30b-5p functions as a metastasis suppressor in colorectal cancer by targeting Rap1b. Cancer Lett 2020;477:144–56.
[41] Jiang WS, Huang CL, Zhang J, et al. MicroRNA-149 inhibits the progression of lung adenocarcinoma through targeting RAP1B and inactivating Wnt/(-catenin pathway. Eur Rev Med Pharmacolog Sci 2020;24:4846–54.
[42] Zhou Z, Xu H, Duan Y, et al. MicroRNA-101 suppresses colorectal cancer progression by negative regulation of Rap1b. Oncology Lett 2020;20:2225–31.
[43] Elfgen C, Reeve K, Moskovszky L, et al. Prognostic impact of PIK3CA protein expression in triple negative breast cancer and its subtypes. J Cancer Res Clin Oncol 2019;145:2051–9.
[44] Zhan S, Wang C, Yin F. MicroRNA-29c inhibits proliferation and promotes apoptosis in non-small cell lung cancer cells by targeting VEGFA. Mol Med Rep 2018;17:6705–10.
[45] Zhang Q, Lei L, Jing D. Knockdown of SERPINE1 reverses resistance of triple-negative breast cancer to paclitaxel via suppression of VEGFA. Oncol Rep 2020;44:1875–84.
[46] Liu Z, Jin H, Yang S, et al. SDC1 knockdown induces epithelial-mesenchymal transition and invasion of gallbladder cancer cells via the ERK/Snail pathway. J Int Med Res 2020;48:300060520947883.
[47] Huff WX, Kwon JH, Henriquez M, et al. The evolving role of CD8 (+) CD28(-) immunosenescent T cells in cancer immunology. Int J Mol Sci 2019;20:
[48] Heimberger AB, Abou-Ghazal M, Reina-Ortiz C, et al. Incidence and prognostic impact of FoxP3+ regulatory T cells in human gliomas. Clin Cancer Res 2008;14:5166–72.
[49] Alexiou GA, Vartholomatos G, Karamoutsios A, et al. Circulating progenitor cells: a comparison of patients with glioblastoma or meningioma. Acta Neurol Belg 2013;113:7–11.
[50] Mu L, Yang C, Gao Q, et al. CD4+ and Perivascular Foxp3+ T Cells in Glioma Correlate with Angiogenesis and Tumor Progression. Front Immunol 2017;8:1451.
[51] Zhong QY, Fan EX, Feng GY, et al. A gene expression-based study on immune cell subtypes and glioma prognosis. BMC Cancer 2019; 19:1116.

[52] Grabowski MM, Sankey EW, Ryan KJ, et al. Immune suppression in gliomas. J Neurooncol 2021;151:3–12. doi:10.1007/s11060-020-03483-y.
[53] Roufas C, Chasiotis D, Makris A, et al. The expression and prognostic impact of immune cytolytic activity-related markers in human malignancies: a comprehensive meta-analysis. Front Oncol 2018;8:27.
[54] Nan Y, Guo H, Guo L, et al. MiRNA-451 inhibits glioma cell proliferation and invasion through the mTOR/HIF-1(/VEGF signaling pathway by targeting CAB39. Hum Gene Therapy Clin Develop 2018;29:156–66.
[55] Sun J, Chen Z, Xiong J, et al. MicroRNA-422a functions as a tumor suppressor in glioma by regulating the Wnt/(-catenin signaling pathway via RPN2. Oncol Rep 2020;44:2108–20.
[56] Luo Y, Zeng G, Wu S. Identification of microenvironment-related prognostic genes in bladder cancer based on gene expression profile. Front Genet 2019;10:1187.